MATEC Web of Conferences **18**, 01002 (2014)
DOI: 10.1051/matecconf/ 20141801002

THREE-DIMENSIONAL RECONSTRUCTION OF A GAS BUBBLE TRAJECTORY IN LIQUID

Jakub Augustyniak[1,a], Dariusz Perkowski[1] and Romuald Mosdorf [1]

[1] Bialystok University of Technology, Faculty of Mechanical Engineering, Wiejska 45C, 15-351 Białystok, Poland, tel. +48 85 746 92 00, fax. +48 85 746 92 10

Abstract. The identification of the shape of the bubble trajectory is crucial for understanding the mechanism of bubble motion in liquid. In the paper it has been presented the technique of 3D bubble trajectory reconstruction using a single high speed camera and the system of mirrors. In the experiment a glass tank filled with distilled water was used. The nozzle through which the bubbles were generated was placed in the centre of the tank. The movement of the bubbles was recorded with a high speed camera, the Phantom v1610 at a 600 fps. The techniques of image analysis has been applied to determine the coordinates of mass centre of each bubble image. The 3D trajectory of bubble can be obtained by using triangulation methods. In the paper the measurement error of imaging computer tomography has been estimated. The maximum measurement error was equal to ±0,65 [mm]. Trajectories of subsequently departing bubbles were visualized.

1 Introduction

With the increase of the bubbles diameter the shapes of bubbles paths change [1]. The shapes of bubble paths are also modified by hydrodynamic interactions between bubbles. The rectilinear path appears when the bubble diameter < 0.81 [mm], the bubble zigzag motion is observed when bubble diameter is 0.81-0.88 [mm] and a bubble spiral motion appears for bubble diameter greater than 1.10 [mm] [2]. Many invasive and non-invasive methods have been presented in the former articles [3-6]. The most interesting ones were: tomography [3], ultrasonic measurement [4], high speed photography [5], PIV system [6]. In the papers [1-6] the trajectory of single bubble were reconstructed.

The main aim of the present paper was to assess the suitability of the imaging computer tomography method for determining the 3D gas bubble trajectory in liquid. It has been analysed the trajectory of subsequently departing bubbles.

The analysis of mutual relationship between the trajectories of subsequently departing bubbles can be useful for estimation of the strengthens of the hydrodynamic interaction between bubbled as a function of frequency of bubble departures.

It has been used the system of mirrors (proposed by C.D. Ohl, A. Tijink and A. Prosperetti [7]) and a single high speed camera. Recorded images have been processed using the following methods: the noise reduction, the image smoothing and the edge detection. The obtained bubble contour was filled with white pixels, and the position of the centre of area of bubble images was calculated. The triangulation transformations were used for calculation of 3D bubble coordinates. The measurement error has been estimated.

2 Experimental setup and data analysis

The experiment was conducted in a glass tank (300 x 150 x 500 mm) filled with distilled water. Figure 1 illustrates the schema of the experimental setup.

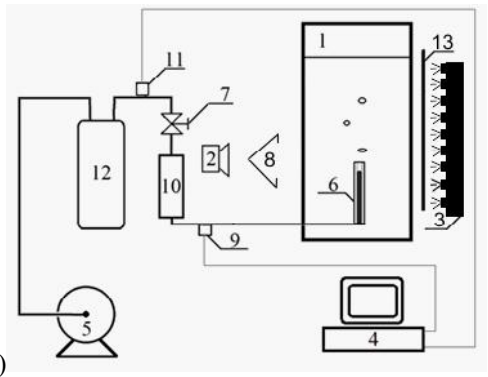

Figure 1. Scheme of the experimental setup a) system configuration, b) three mirror system: 1 – glass tank, 2 – camera, 3 – light panel, 4 – data acquisition station, 5 – air pump, 6 – nozzle, 7 – air valve, 8 – mirrors, 9,11 – pressure sensor, 10 – flow meter, 12 – air tank.

[a] Corresponding author: jak.august@gmail.com

Through an air valve the air was delivered to a flow meter. This way the air was provided into a brass nozzle with an internal diameter of 1.1 mm and 7 mm in length placed in the centre of the tank bottom. The video was recorded with a high speed camera Phantom v1610 with 600 fps. The glass tank was illuminated from both sides by LED panels. To disperse the light the "milk" glass was used. A three mirror system was used which gave the possibility to obtain two different projections of the same scene on the one single frame recorded with the camera. For this purpose two flat mirrors were placed on the sides of the glass tank. The reflected projections were focused by the rectangular third mirror.

The image analysis has been prepared by a computer program with using the OpenCV library. The frames were blurred and the noise reduced. For this purpose a median filter was used. The Canny edge filter has been used for bubble edge detection. The edge finding process started from the convolution between the non-noise image with two 3x3 matrixes in order to determine the intensity gradient of the image. The used matrixes were [8]:

$$G_x = \begin{bmatrix} -1 & 0 & 1 \\ -2 & 0 & 2 \\ -1 & 0 & 1 \end{bmatrix}, \tag{1}$$

$$G_y = \begin{bmatrix} -1 & -2 & -1 \\ 0 & 0 & 0 \\ 1 & 2 & 1 \end{bmatrix}, \tag{2}$$

$$G = \sqrt{G_x^2 + G_y^2}\ . \tag{3}$$

Next two thresholds (upper and lower) are setup. When the pixels brightness is below the lower threshold, the pixel is not considered. When the brightness is higher than the upper threshold, the pixel is treated as belonging to the edge. When the pixel brightness is between the upper and the lower threshold, the pixel is treated as belonging to the edge when at least one of its neighbours belongs to the edge.

The reconstruction of the bubble trajectory required the finding of the centre of area of a bubble images in each frame. The position of the centre of bubble area is defined as follows:

$$x_c = \frac{S_y}{A} = \frac{\iint_A x dA}{\iint_A dA} = \frac{\iint_A x dx dy}{\iint_A dx dy}, \tag{4}$$

$$y_c = \frac{S_x}{A} = \frac{\iint_A y dA}{\iint_A dA} = \frac{\iint_A y dx dy}{\iint_A dx dy}, \tag{5}$$

where: x_c- centre of area in the x axis; y_c - centre of mass in the y axis; S_x, S_y - moment of inertia corresponding to the x and y axes, respectively; A- figure surface area.

The obtained bubble contour was filled with white pixels and the position of the centre of area of bubble images was calculated. For determining the bubble displacements the Kalman filter was used [9]. The bubble location was sought by means of ROI (Region of Interest), which moved simultaneously with the gas bubble.

In Figure 2 it has been presented the subsequent steps of image processing. Figure 2a shows the recorded image after the blurring and noise reduction (1-left projection, 2-right projection). Figure 2b is the result of the Canny edge filter, Figure 2c presents the ROI and a completely filled contour. Figure 2d shows the centre of bubble image area.

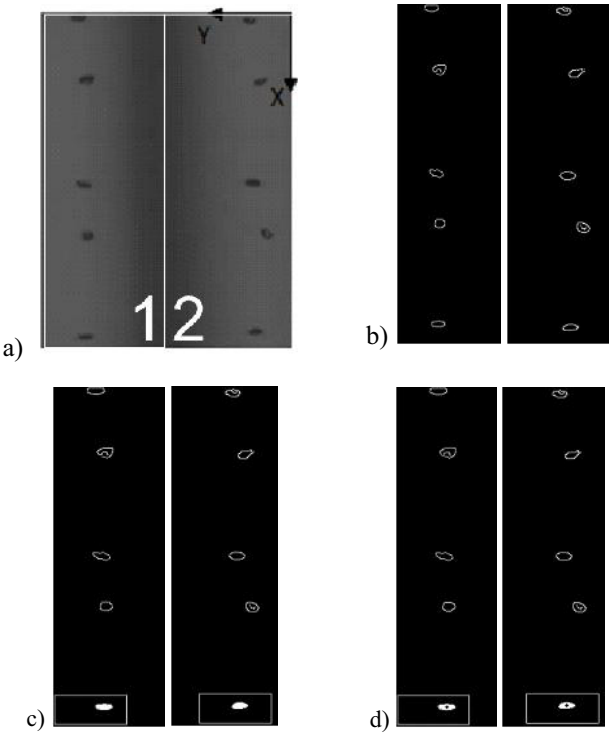

Figure 2. Steps of determining the mass centre of gas bubbles: a) image submitted for blurring, b) the effect of Canny edge filter, c) filling of contours found in ROI, d) example of centre of area of bubble images inside the ROI.

3 Triangulation

The bubble coordinates in the coordinates system which origin is located in the nozzle outlet have been calculated according the following formulas:

$$X_c = \frac{\sin(\frac{3\pi}{4} - \beta)\sin(\alpha)\cos(\frac{\pi}{2} - \alpha)x}{\sin(\beta)\sin(\frac{3\pi}{4} - \alpha)}, \tag{6}$$

$$Y_c = \frac{\sin(\frac{3\pi}{4}-\beta)\sin(\alpha)\cos(\frac{\pi}{2}-\alpha)y}{\sin(\beta)\sin(\frac{3\pi}{4}-\alpha)}, \qquad (7)$$

$$Z_c = Rk - \frac{Pp_1 + Pp_2}{2} - \frac{Sp_1 + Sp_2}{2}. \qquad (8)$$

Figure 3 presents the visual interpretation of triangulation transformations for X_c. The α and β are the angles which are measured as it has been shown in Figure 3. X_c and Y_c are the coordinates in the coordinates system whose origin is located at the nozzle outlet.

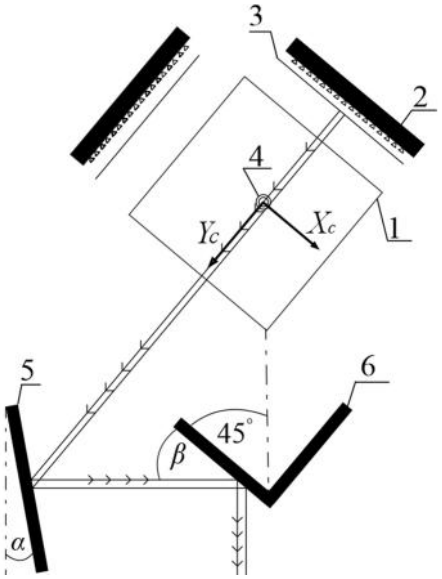

Figure 3. Visual interpretation of triangulation transformation for X_c. (1 – glass tank, 2 – LED panel, 3 – „milk" glass, 4 – nozzle, 5,6 – mirrors).

4 Measurement error

Measurement of position of the centre of area was an indirect measurement. To determine the accuracy of the measurement method, the total differential method was used [10]. The estimation of the errors ΔX_c and ΔY_c has been made using the following formulas:

$$\Delta X_c = \frac{\partial}{\partial\alpha}X_c(\alpha,\beta,x)\Delta\alpha + \frac{\partial}{\partial\beta}X_c(\alpha,\beta,x)\Delta\beta + \frac{\partial}{\partial x}X_c(\alpha,\beta,x)\Delta x, \qquad (9)$$

$$\Delta Y_c = \frac{\partial}{\partial\alpha}Y_c(\alpha,\beta,y)\Delta\alpha + \frac{\partial}{\partial\beta}Y_c(\alpha,\beta,y)\Delta\beta + \frac{\partial}{\partial y}Y_c(\alpha,\beta,y)\Delta y, \qquad (10)$$

$$\Delta Z_c = \frac{\partial}{\partial\delta}Z_c(\delta,z)\Delta\delta + \frac{\partial}{\partial z}Z_c(\delta,z)\Delta z\ . \qquad (11)$$

$\Delta\alpha$ and $\Delta\beta$ are the protractors measurement errors which are equal to 5'. Δx and Δy were estimated based on the comparison between experimental measurement and the known diameter of a metal ball. $\Delta\delta$ is the deviation error of z axis from the 90° vertical line. The maximum error of Δz (in 100 measurements) was less than ±0,5 [mm]. The maximum measurement error defined by the Eq. 9,10,11 was equal to ±0,65 [mm]. These errors significantly depend on the image resolution. In the experiment the image resolution was 1280x800 [pix].

5 Results

The numerical values obtained with using the algorithm described above allowed us to plot the 3D gas bubble trajectories.

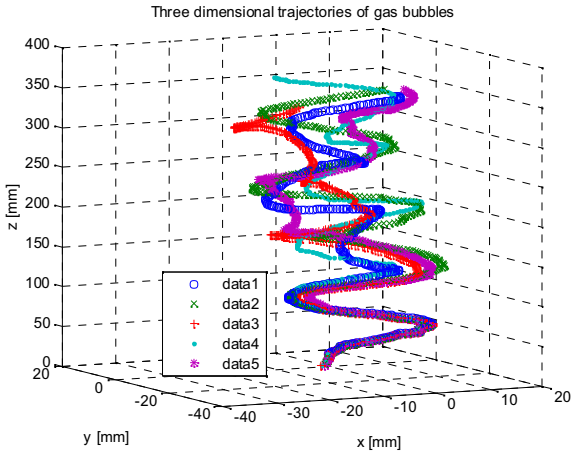

Figure 4. 3D reconstruction of gas bubble trajectories

Figure 4 presents the paths of five bubbles. The maximum lateral bubble displacement was 34 pixels (~19 [mm]). The measurement error mentioned in point 4 was ±0,65 [mm], so the relation: error to maximum amplitude is smaller than 1%. Errors related to the position of mirrors (the $\Delta\alpha$ and $\Delta\beta$) represent only 20% of the maximum measurement error. The remaining 80% is related with the Δx and Δy measurements.

6 Conclusion

In this paper the imaging computer tomography method for the gas bubble has been applied. The videos recorded by the Phantom v1610 camera have been analysed by computer program which used the median blur filter, Canny edge filter and Kalman filter. With using the triangulation techniques the 2D bubble coordinates were transformed into 3D coordinates system. The three dimensional trajectories of bubbles have been reconstructed. The measurement error has been calculated considering the positions of the mirrors. The movies were recorded at 600 fps with a 1280x800 [pix] resolution. In this experiment the maximum measurement error was $\pm 0,65$ [mm]. The most significant contribution in measurement error has the Δx and Δy measurements. Their values significantly depend on the image resolution. The video recorded with a higher resolution

has a smaller error. The improving the accuracy of reconstructed bubble paths can be obtained by increasing the image resolution or using a moving camera.

References

1. W.L. Shew, S.Poncet, J-F. Pinton, J.Fliud Mech., vol. **569**, 51-60, (2006)
2. K. Lunde, R. Perkins, ASME Fluids, FEDSM 3530, (1997)
3. H. Ding, ZY. Song ZH, Flow Meas. Instrum, vol. **18**, 37-46, (2007)
4. S. Wada, H. Kikura, M. Aritomi, Flow Meas, Instrum, vol. **17**, 207-224, (2006)
5. C. Lin, M. Gilberston, A. Harrison, Chem. Eng. Sci, vol **62**, 56-69, (2007)
6. K. Sakakibara, M. Yamada, Y. Miyamoto, Flow. Meas. Instrum, vol. **18**, 211-215, (2007)
7. C.D. Ohl, A.Taijink, A.Prosperetti, J.Fliud Mech., vol. **482**, 271-290, (2003)
8. L. Ding, A. Goshtasby, Pattern Recognition, nr. 34, 721-725, (2001)
9. R.E. Kalman, J. Basic Eng., vol. **82**, no. **1**, (1960)
10. W. Jakubiec, J. Malinowski, *Metrologia wilekości geometrycznych*, Wydawnictwa Naukowo-Techniczne – Wydanie czwarte zmienione, 52-93, (2004)
11. P.C Duineveld, J.Fluid Mech., vol. **292**, 325-332, (1995)
12. A.A. Kulkarni, B.J Jyeshthraja, Ind. Eng. Chem. Res., vol. **44**, (2005)
13. A.W.G. de Vries, A. Biesheuvel, L van Wijngaarde, Int. j. multiph. Flow, vol. **28**, (2002)
14. N.M. Aybers, A. Tapucu, Heat and Mass Transfer, vol. **2**, (1969)
15. N.M.S. Hassan, M.M.K. Khan, M.G. Rasul, Wseas transition on fluid mechanisc, vol. **3**, no.**3**, (2008)
16. K. Ellingsen, F. Risso, J.Fluid Mech., vol. **440**, (2001)